Discontinuous Galerkin methods on unstructured meshes for the numerical resolution of the time-domain Maxwell equations

V. Dolean[1,2] L. Fezoui[2] S. Lanteri[2] F. Rapetti[1,2]

[1]J.A. Dieudonné Mathematics Laboratory, University of Nice/Sophia Antipolis
06108 Nice Cedex, France
[2]INRIA, project-team CAIMAN
2004 Route des Lucioles, BP 93, 06902 Sophia Antipolis Cedex, France

Numelec 2006, Lille, November 29th-30th/December 1st

Content

Numerical methods for the time-domain Maxwell equations
Overview of existing methods

- FDTD: Finite Difference Time-Domain method
- Seminal work of K.S. Yee
  (IEEE Trans. Antennas Propag., Vol. AP-14, 1966)
- Structured (cartesian) meshes
- Second order accurate (space and time) on uniform meshes
- Advantages
  - Easy computer implementation
  - Computationally efficient (very low algorithmic complexity)
  - Mesh generation is straightforward
  - Modelization of complex sources (antennas, thin wires, etc.) is well established
- Drawbacks
  - Accuracy on non-uniform discretizations
  - Memory requirements for high resolution models
  - Approximate discretization of boundaries (stair case representation)

- FETD: Finite Element Time-Domain method
- Often based on J.-C. Nédélec edge elements (Numer. Math, Vol. 35, 1980 and Vol. 50, 1986)
  - Unstructured meshes
  - Advantages
    - Accurate representation of complex shapes
    - Well suited to high order interpolation methods
  - Drawbacks
    - Computer implementation is less trivial
    - Unstructured mesh generation is hardly automated
    - Global mass matrix
  - Mass lumped FETD methods
    - S. Pernet, X. Ferrieres and G. Cohen
IEEE Trans. Antennas Propag., Vol. 53, No. 9, 2005
    - Hexahedral meshes, high order Lagrange polynomials
    - Leap-frog time integration scheme

- FVTD: Finite Volume Time-Domain method
  - Imported from the CFD community
    - V. Shankar, W. Hall and A. Mohammadian
      Electromag. Vol. 10, 1990
    - J.-P. Cioni, L. Fezoui and H. Steve
      IMPACT Comput. Sci. Eng., Vol. 5, No. 3, 1993
    - P. Bonnet, X. Ferrieres *et al.*
      J. Electromag. Waves and Appl., Vol. 11, 1997
    - S. Piperno and M. Remaki and L. Fezoui
      SIAM J. Num. Anal., Vol. 39, No. 6, 2002.
  - Unstructured meshes
  - Uknowns are cell averages of the field components
  - Flux evaluation at cell interfaces
    - Upwind scheme $\longrightarrow$ numerical dissipation
    - Centered scheme $\longrightarrow$ numerical dispersion (on non-uniform meshes)
  - Extension to higher order accuracy: MUSCL technique

- Numerical modelling methodology on unstructured simplicial meshes
- Accuracy
  - High-order polynomial interpolation
  - Low level of numerical dispersion on locally refined meshes
- Stability
  - Non-dissipative (long time behavior)
- Flexibility
  - Non-conforming meshes
  - *hp*-adaptivity
- Numerical efficiency
  - Locally implicit time-stepping
- Computational efficiency
  - Parallel computing platforms
  - High performance linear algebra kernels (BLAS)

Discontinuous Galerkin methods

Some generalities

- Initially introduced to solve neutron transport problems (W. Reed and T. Hill, 1973)
- Became popular as a framework for solving hyperbolic or mixed hyperbolic/parabolic problems
- Recently developed for elliptic problems
- Somewhere between a finite element and a finite volume method, gathering many good features of both
- Main properties
  - Can easily deal with discontinuous coefficients and solutions
  - Can handle unstructured, non-conforming meshes
  - Yield local finite element mass matrices
  - High-order accurate methods with compact stencils
  - Naturally lead to discretization and interpolation order adaptivity
  - Amenable to efficient parallelization

- Problem to solve

  $\mathbf{x} \in \Omega \subset \boldsymbol{R}^d,\ t \in \boldsymbol{R}^+$, $u = u(\mathbf{x}, t)$, $a_i = a_i(\mathbf{x})$ scalar real functions

$$\frac{\partial u}{\partial t} + \sum_{i=1}^{d} a_i \frac{\partial u}{\partial x_i} = 0$$

- Weak formulation

$$< \frac{\partial u}{\partial t},\ v >_\Omega + \sum_{i=1}^{d} < a_i \frac{\partial u}{\partial x_i},\ v >_\Omega = 0$$

$< u\ ,\ v >_\Omega = \int_\Omega uvd\mathbf{x}$, v being a *test function*

Discontinuous Galerkin time-domain methods
Basic principles

- Galerkin method
  - $\tau_h = \{K\}$ triangulation of Ω
  - $\mathbb{P}_p(K)$: polynomials of degree at most p on K

For each $K \in \tau_h$ find $u^h : u^h|_K \in \mathbb{P}_p(K)$ such that:

$$< \frac{\partial u^h}{\partial t}, \ v >_K + \sum_{i=1}^{d} < a_i \frac{\partial u^h}{\partial x_i}, \ v >_K = 0 \ \ , \forall v \in \mathbb{P}_p(K)$$

Integrating by parts (setting $a|_K \in \mathbb{P}_0(K)$)

$$\begin{aligned} < \frac{\partial u^h}{\partial x_i}, \ v >_K &= - < u^h, \ \frac{\partial v}{\partial x_i} >_K + < u^h n_i, \ v >_{\partial K} \\ < u, \ v >_{\partial K} &= \sum_{j=1}^{N_f(K)} < u, \ v >_{\partial K \cap \partial K_j} \end{aligned}$$

- $\mathbf{n} = \{n_i\}$ outward unit normal of ∂K
- $N_f(K)$ = number of faces of K

- Discontinous approximation: $u^h|_{K\cap K_j}$ not well defined!
- Linear algebra
  - $u^h|_K(\mathbf{x},t) = \sum_{j=1}^{p_K} u^h_{j,K}(t)\psi_{j,K}(\mathbf{x})$, $p_K = \dim(\mathbb{P}_p(K))$
  - $\{\psi_{j,K}\}, j = 1,\dots,p_K$: basis of $\mathbb{P}_p(K)$

$$\mathbf{M}_K \frac{\partial \mathbf{U}^h_K}{\partial t} = \sum_{i=1}^{d} a_i \left(\mathbf{R}_{i,K}\mathbf{U}^h_K - n_i \sum_{j=1}^{N_f(K)} \mathbf{S}_{K,K_j}\mathbf{U}^h_K \right)$$

$$\begin{aligned}
\mathbf{U}^h_K \quad &= \quad \mathbf{U}^h_K(t) = \{u^h_{j,K}(t)\}, \quad j = 1,\dots,p_K \\
\mathbf{M}_K[l,p] \quad &= \quad <\psi_{l,K},\ \psi_{p,K}>_K \\
\mathbf{R}_{i,K}[l,p] \quad &= \quad <\frac{\partial \psi_{l,K}}{\partial x_i},\ \psi_{p,K}>_K \\
\mathbf{S}_{K,K_j}[l,p] \quad &= \quad <\psi_{l,K},\ \psi_{p,K_j}>_{\partial K\cap\partial K_j}
\end{aligned}$$

Dimension of local systems: $p_K \times p_K$

Discontinuous Galerkin methods for the Maxwell equations
Related works

- F. Bourdel, P.A. Mazet and P. Helluy
  Proc. 10th Inter. Conf. on Comp. Meth. in Appl. Sc. and Eng., 1992.
  - Triangular meshes, first-order upwind DG method (i.e FV method)
  - Time-domain and time-harmonic Maxwell equations
- M. Remaki and L. Fezoui, INRIA RR-3501, 1998.
  - Time-domain Maxwell equations
  - Triangular meshes, P1 interpolation, Runke-Kutta time integration (RKDG)
- J.S. Hesthaven and T. Warburton (J. Comput. Phys., Vol. 181, 2002)
  - Tetrahedral meshes, high order Lagrange polynomials, upwind flux
  - Runge-Kutta time integration
- B. Cockburn, F. Li and C.-W. Shu (J. Comput. Phys., Vol. 194, 2004)
  - Locally divergence-free RKDG formulation
- G. Cohen, X. Ferrieres and S. Pernet (J. Comput. Phys., Vol. 217, 2006)
  - Hexahedral meshes, high order Lagrange polynomials, penalized formulation
  - Leap-frog time integration scheme

$$\left\{\begin{array}{lcccc} \varepsilon(\mathbf{x})\dfrac{\partial \mathbf{E}}{\partial t} & - & \nabla \times \mathbf{H} & = & -\mathbf{J} \\ \mu(\mathbf{x})\dfrac{\partial \mathbf{H}}{\partial t} & + & \nabla \times \mathbf{E} & = & 0 \end{array}\right.$$

- $\mathbf{E} = \mathbf{E}(\mathbf{x}, t)$: electric field
- $\mathbf{H} = \mathbf{H}(\mathbf{x}, t)$: magnetic field
- $\varepsilon(\mathbf{x})$: electric permittivity
- $\mu(\mathbf{x})$: magnetic permeability
- $\mathbf{J} = \mathbf{J}(\mathbf{x}, t)$: electric current density
  - Conductive media: $\mathbf{J} = \sigma \mathbf{E}$
  - $\sigma(\mathbf{x})$: electric conductivity

- Face: $a_{ik} = \tau_i \cap \tau_k$, $\mathcal{V}_i = \{k \ \text{ with } \ \tau_k \ \text{ such that } \ \tau_i \cap \tau_k \neq \emptyset\}$
- Centered fluxes, leap-frog time integration
- L. Fezoui and S. Piperno, INRIA research report No. 4733, 2003

$$\left\{ \begin{array}{lcl} \displaystyle\iiint_{\tau_i} \vec{\varphi} \cdot \varepsilon_i \left(\frac{\mathbf{E}_i^{n+1} - \mathbf{E}_i^n}{\Delta t} \right) d\omega & = & \displaystyle -\sum_{k \in \mathcal{V}_i} \Phi_{H,ik}^{n+\frac{1}{2}} + \iiint_{\tau_i} \nabla \times \vec{\varphi} \cdot \mathbf{H}_i^{n+\frac{1}{2}} d\omega \\ \displaystyle\iiint_{\tau_i} \vec{\varphi} \cdot \mu_i \left(\frac{\mathbf{H}_i^{n+\frac{3}{2}} - \mathbf{H}_i^{n+\frac{1}{2}}}{\Delta t} \right) d\omega & = & \displaystyle \sum_{k \in \mathcal{V}_i} \Phi_{E,ik}^{n+1} - \iiint_{\tau_i} \nabla \times \vec{\varphi} \cdot \mathbf{E}_i^{n+1} d\omega \end{array} \right.$$

$$\text{with :} \quad \left\{ \begin{array}{lcl} \Phi_{H,ik}^{n+\frac{1}{2}} & = & \displaystyle\iint_{a_{ik}} \vec{\varphi} \cdot \left(\frac{\mathbf{H}_i^{n+\frac{1}{2}} + \mathbf{H}_k^{n+\frac{1}{2}}}{2} \right) \times \vec{n}_{ik} d\sigma \\ \Phi_{E,ik}^{n+1} & = & \displaystyle\iint_{a_{ik}} \vec{\varphi} \cdot \left(\frac{\mathbf{E}_i^{n+1} + \mathbf{E}_k^{n+1}}{2} \right) \times \vec{n}_{ik} d\sigma \end{array} \right.$$

- Approximation space: $V_h = \{\mathbf{V}_h \in L^2(\Omega)^3 \mid \forall i, \mathbf{V}_{h|\tau_i} \equiv \mathbf{V}_i \in \mathbb{P}_p(\tau_i)^3\}$

$$\mathbf{E}_i^n(\mathbf{x}) = \sum_{1\leq j\leq d_i} E_{ij}^n \vec{\varphi}_{ij}(\mathbf{x}) \quad \text{and} \quad \mathbf{H}_i^{n+\frac{1}{2}}(\mathbf{x}) = \sum_{1\leq j\leq d_i} H_{ij}^{n+\frac{1}{2}} \vec{\varphi}_{ij}(\mathbf{x})$$

- $\mathbb{E}_i^n = \{E_{ij}^n\}_{1\leq j\leq d_i}$ and $\mathbb{H}_i^{n+\frac{1}{2}} = \{H_{ij}^{n+\frac{1}{2}}\}_{1\leq j\leq d_i}$
- $\mathbf{M}_i^{\varepsilon} = \varepsilon_i \iiint_{\tau_i} {}^{\mathsf{T}}\vec{\varphi}_{ij}\vec{\varphi}_{ij} d\omega$ and $\mathbf{M}_i^{\mu} = \mu_i \iiint_{\tau_i} {}^{\mathsf{T}}\vec{\varphi}_{ij}\vec{\varphi}_{ij} d\omega$

$$1 \leq j \leq d_i \quad : \quad \left\{ \begin{array}{rl} \left[\mathbf{M}_i^{\varepsilon}\left(\dfrac{\mathbb{E}_i^{n+1} - \mathbb{E}_i^n}{\Delta t}\right)\right]_j & = -\displaystyle\sum_{k\in\mathcal{V}_i} \mathbf{\Phi}_{H,ik}^{n+\frac{1}{2}} + \iiint_{\tau_i} \nabla \times \vec{\varphi}_{ij} \cdot \mathbf{H}_i^{n+\frac{1}{2}} d\omega \\ \left[\mathbf{M}_i^{\mu}\left(\dfrac{\mathbb{H}_i^{n+\frac{3}{2}} - \mathbb{H}_i^{n+\frac{1}{2}}}{\Delta t}\right)\right]_j & = \displaystyle\sum_{k\in\mathcal{V}_i} \mathbf{\Phi}_{E,ik}^{n+1} - \iiint_{\tau_i} \nabla \times \vec{\varphi}_{ij} \cdot \mathbf{E}_i^{n+1} d\omega \end{array} \right.$$

- Theoretical aspects
  - L. Fezoui, S. Lanteri, S. Lohrengel and S. Piperno
    M2AN, Vol. 39, No. 6, 2005
  - Stability through the conservation of a discrete electromagnetic energy

$$\mathcal{E}^n = \frac{1}{2}\sum_i \iiint_{\tau_i} \left({}^{\mathsf{T}}(\mathbf{E}_i^n)\varepsilon_i \mathbf{E}_i^n + {}^{\mathsf{T}}(\mathbf{H}_i^{n-\frac{1}{2}})\mu_i \mathbf{H}_i^{n+\frac{1}{2}} \right)$$

  - CFL condition (V_i and P_i: volume and perimeter of τ_i)

$$\forall i,\ \forall k \in \mathcal{V}_i\ : c_i \Delta t \left[2\alpha_i + \beta_{ik} \max\left(\sqrt{\frac{\mu_i}{\mu_k}, \frac{\varepsilon_i}{\varepsilon_k}} \right) \right] < \frac{4V_i}{P_i},$$

    where α_i and β_{ik} are dimensionless coefficients, independent of h
  - Convergence of the fully discrete $\mathbb{P}_p$-DGTD method

$$\mathcal{O}(Th^{\min(s,p)}) + \mathcal{O}(\Delta t^2)$$

    for the total error in $C^0([0,T];L^2(\Omega))$ with $s > \frac{1}{2}$ a regularity parameter

- Tetrahedral meshes
- Nodal (Lagrange) basis functions
  - $\mathbb{P}_0$-DGTD method
    - Centered finite volume method, 6 dof per tetrahedron
    - S. Piperno and M. Remaki and L. Fezoui
      SIAM J. Num. Anal., Vol. 39, No. 6, 2002.
  - $\mathbb{P}_1$-DGTD method: 24 dof per tetrahedron
  - $\mathbb{P}_2$-DGTD method: 60 dof per tetrahedron
  - $\mathbb{P}_3$-DGTD method: 120 dof per tetrahedron
- Parallel computing aspects
  - SPMD parallelization strategy
    - Mesh partitioning (ParMeTiS)
    - Message passing programming model (MPI)
  - M. Bernacki and S. Lanteri and S. Piperno
    J. Comp. Acoustics, Vol. 14, No. 1, 2006.

- Eigenmode in a spherical metallic cavity (R=1, F=131 MHz)
  - Mesh M1: # vertices = 14,993 , # tetrahedra = 81,920
  - $L_{\text{min}} = 0.0625$ m , $L_{\text{max}} = 0.2473$ m $(\approx \dfrac{\lambda}{9})$, $L_{\text{avg}} = 0.0875$ m

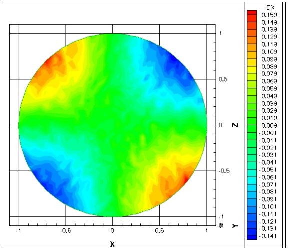

$\mathbb{P}_0$-DGTD method
CFL=1.00 , CPU= 75 sec

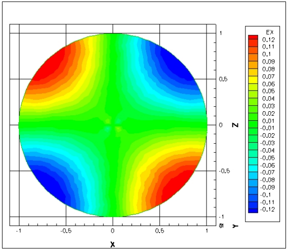

$\mathbb{P}_1$-DGTD method
CFL=0.33 , CPU= 597 sec

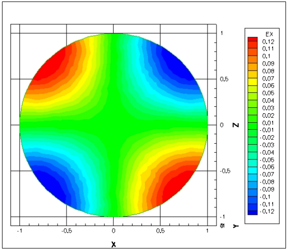

$\mathbb{P}_2$-DGTD method
CFL=0.16 , CPU=3732 sec

Contour lines of E_x in the plane $Y = 0$
AMD Opteron 2 GHz, Gigabit Ethernet, # procs = 4

- Eigenmode in a spherical metallic cavity (R=1, F=131 MHz)
  - Mesh M2: # vertices = 2,057 , # tetrahedra = 10,240
  - $L_{\min} = 0.1250$ m , $L_{\max} = 0.3703$ m $(\approx \dfrac{\lambda}{6})$, $L_{\text{avg}} = 0.1678$ m

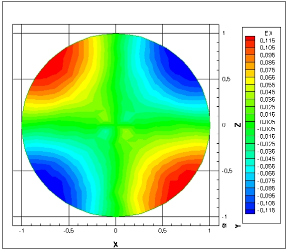

$\mathbb{P}_1$-DGTD method
CFL=0.33 , CPU= 64 sec

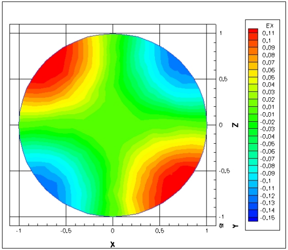

$\mathbb{P}_2$-DGTD method
CFL=0.16 , CPU=423 sec

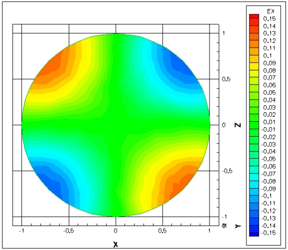

$\mathbb{P}_3$-DGTD method
CFL=0.16 , CPU=920 sec

Contour lines of E_x in the plane $Y = 0$
AMD Opteron 2 GHz, Gigabit Ethernet, # procs = 1

- Eigenmode in a spherical metallic cavity (R=1, F=131 MHz)

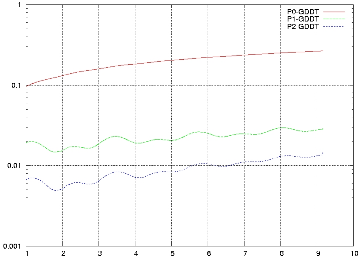

Mesh M1
vertices = 14,993 , # tetrahedra = 81,920

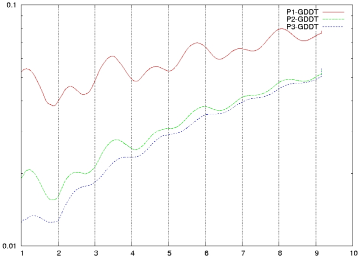

Mesh M2
vertices = 2,057 , # tetrahedra = 10,240

Time evolution of the L^2 norm of the error

- Eigenmode in a spherical metallic cavity (R=1, F=131 MHz)

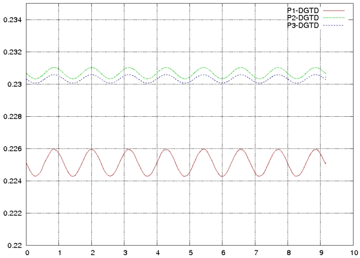

Mesh M1
\# vertices = 14,993 , # tetrahedra = 81,920

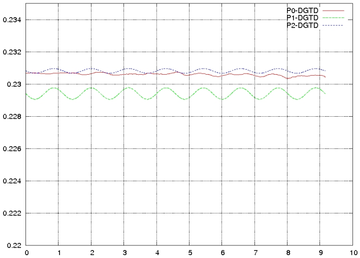

Mesh M2
\# vertices = 2,057 , # tetrahedra = 10,240

Time evolution of the discrete electromagnetic energy

- Diffraction of a plane wave by a PEC sphere, F=300 MHz

Mesh	# vertices	# tetrahedra	$L_{\min}$ (m)	$L_{\max}$ (m)	L_{moy} (m)
M1	4,624	24,192	0.1228	0.5215	0.2648
M2	10,260	55,296	0.0942	0.4058	0.2007
M3	21,192	116,424	0.0747	0.3209	0.1560

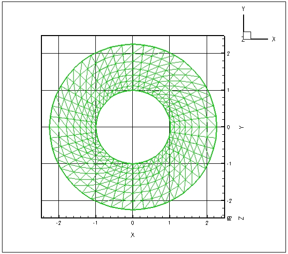

Mesh M1

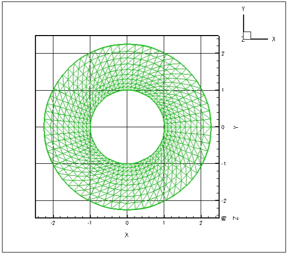

Mesh M2

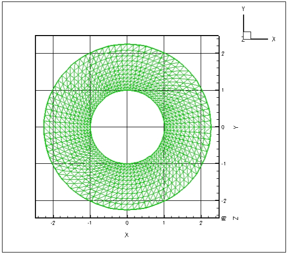

Mesh M3

- Diffraction of a plane wave by a PEC sphere, F=300 MHz
  - Mesh M1: # vertices = 4,624 , # tetrahedra = 24,192
  - $L_{\min} = 0.1228$ m , $L_{\max} = 0.5215$ m ($\approx \dfrac{\lambda}{2}$) , $L_{\text{avg}} = 0.2648$ m

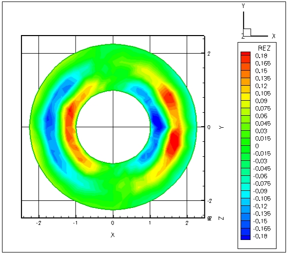

$\mathbb{P}_1$-DGTD method
CPU= 80 sec

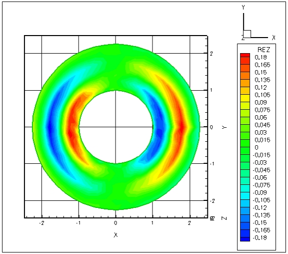

$\mathbb{P}_2$-DGTD method
CPU=260 sec

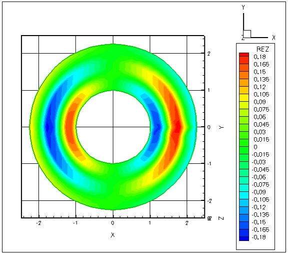

$\mathbb{P}_3$-DGTD method
CPU=738 sec

Contour lines of the real part of DFT(E_z)
Intel Centrino dual-core 2 GHz, # procs = 2

- Diffraction of a plane wave by a PEC sphere, F=300 MHz
  - Mesh M2: # vertices = 10,260 , # tetrahedra = 55,296
  - $L_{\text{min}} = 0.0942$ m , $L_{\text{max}} = 0.4058$ m $(\approx \dfrac{\lambda}{2.5})$, $L_{\text{avg}} = 0.2007$ m

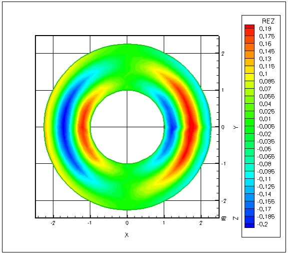

$\mathbb{P}_1$-DGTD method
CPU= 490 sec

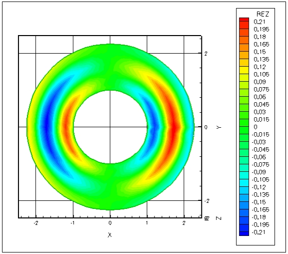

$\mathbb{P}_2$-DGTD method
CPU= 890 sec

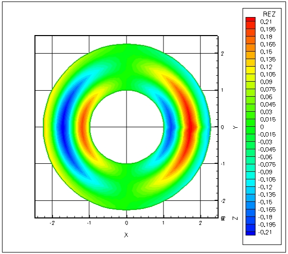

$\mathbb{P}_3$-DGTD method
CPU=4040 sec

Contour lines of the real part of DFT(E_z)
Intel Centrino dual-core 2 GHz, # procs = 2

- Diffraction of a plane wave by a PEC sphere, F=300 MHz
  - Mesh M2: # vertices = 21,192 , # tetrahedra = 116,424
  - $L_{\text{min}} = 0.0747$ m , $L_{\text{max}} = 0.3209$ m $(\approx \frac{\lambda}{9})$, $L_{\text{avg}} = 0.1560$ m

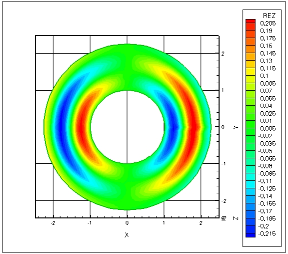

$\mathbb{P}_1$-DGTD method
CPU= 644 sec

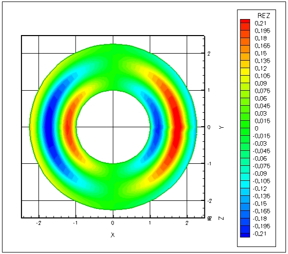

$\mathbb{P}_2$-DGTD method
CPU=1437 sec

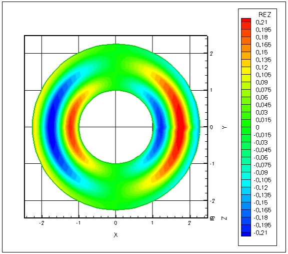

$\mathbb{P}_3$-DGTD method
CPU=6057 sec

Contour lines of the real part of DFT(E_z)
Intel Centrino dual-core 2 GHz, # procs = 2

- Diffraction of a plane wave by a PEC sphere, F=300 MHz
    - Mesh M1: # vertices = 4,624 , # tetrahedra = 24,192
    - $L_{\min} = 0.1228$ m , $L_{\max} = 0.5215$ m $(\approx \dfrac{\lambda}{2})$, $L_{\text{avg}} = 0.2648$ m

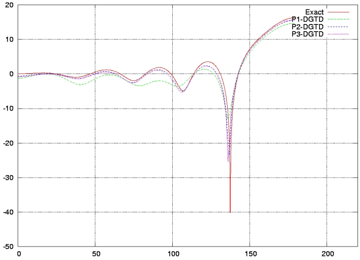

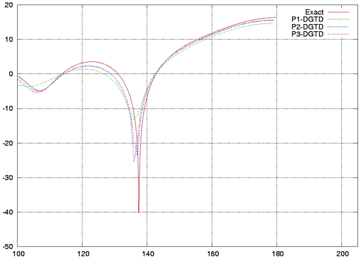

- Diffraction of a plane wave by an aircraft, F=1 GHz
  - Mesh M1: # vertices = 75,200 , # tetrahedra = 423,616
  - $L_{\mathrm{min}} = 0.000601$ m , $L_{\mathrm{max}} = 0.144679$ m $(\approx \dfrac{\lambda}{0.5})$, $L_{\mathrm{avg}} = 0.041361$ m

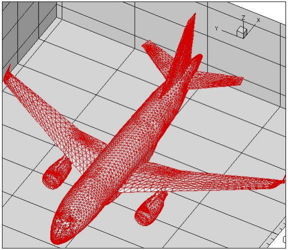

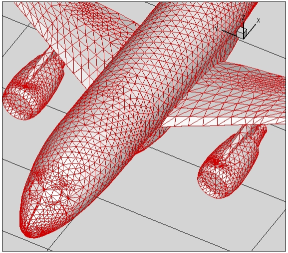

- Diffraction of a plane wave by an aircraft, F=1 GHz
  - Mesh M1: # vertices = 75,200 , # tetrahedra = 423,616
  - $L_{\min} = 0.000601$ m , $L_{\max} = 0.144679$ m $(\approx \dfrac{\lambda}{0.5})$, $L_{\text{avg}} = 0.041361$ m

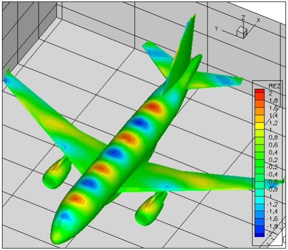

$\mathbb{P}_1$-DGTD method

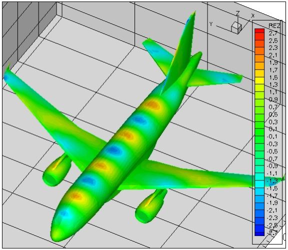

$\mathbb{P}_2$-DGTD method

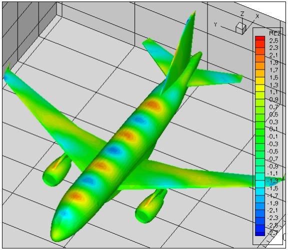

$\mathbb{P}_3$-DGTD method

Contour lines of the real part of DFT(E_z)

- Diffraction of a plane wave by an aircraft, F=1 GHz
    - AMD Opteron 2 GHz, Gigabit Ethernet

Method	N_p	CPU (min/max)	REAL	% CPU
$\mathbb{P}_1$-DGTD	32	38 mn/38 mn	40 mn	98.5%
$\mathbb{P}_2$-DGTD	32	2 h 20 mn/2 h 33 mn	2 h 35 mn	98.5%
$\mathbb{P}_3$-DGTD	32	4 h 49 mn/5 h 08 mn	5 h 12 mn	99.0%

Realistic numerical modelling of mobile phone radiation

HeadExp: realistic numerical modelling of human HEAD tissues EXPosure to electromagnetic waves radiation from mobile phones

- A multi-disciplinary cooperative research action
  - From January 2003 to December 2004
  - Partners: INRIA, ENST Paris, INERIS et FT R&D
- Objectives
  - Contribute to ongoing research activities on biological effects resulting from the use of mobile phones
  - Demonstrate the benefits of using unstructured mesh Maxwell solvers for numerical dosimetric studies
  - Evaluate the thermal effects induced by the electromagnetic radiation in head tissues
- Specific activities
  - Medical image processing (segmentation of head tissues)
  - Geometrical modelling (surface and volumic mesh generation)
  - Numerical modelling (time domain Maxwell solvers, bioheat equation solver)
  - Experimental validations

HeadExp collaborative research action

Characteristics of tissues (F=1.8 GHz)

Tissue	ε_r	σ (S/m)	ρ (Kg/m^3)	λ (mm)
Skin	43.85	1.23	1100.0	26.73
Skull	15.56	0.43	1200.0	42.25
CSF	67.20	2.92	1000.0	20.33
Brain	43.55	1.15	1050.0	25.26

- Geometrical models
  - Built from segmented medical images
  - Collaboration with INRIA teams specialized in medical image processing and geometrical modelling
  - Extraction of surfacic (triangular) meshes of the tissue interfaces using specific tools
    - Marching cubes + adaptive isotropic surface remeshing (P. Frey, 2001)
    - Delaunay refinement (J.-D. Boissonnat and S. Oudot, 2005)
    - Level-set method (J.-P. Pons, 2005)
  - Generation of tetrahedral meshes using a Delaunay/Voronoi tool

HeadExp collaborative research action

Characteristics of unstructured meshes of head tissues

- Coarse mesh (M1)
  - # vertices = 135,633 and # tetrahedra = 781,742

Tissue	L_{min} (mm)	L_{max} (mm)	L_{avg} (mm)	λ (mm)
Skin	1.339	8.055	4.070	26.73
Skull	1.613	7.786	4.069	42.25
CSF	0.650	7.232	4.059	20.33
Brain	0.650	7.993	4.009	25.26

- Fine mesh (M2)
  - # vertices = 889,960 and # tetrahedra = 5,230,947

Tissue	L_{min} (mm)	L_{max} (mm)	L_{avg} (mm)	λ (mm)
Skin	0.821	5.095	2.113	26.73
Skull	0.776	4.265	2.040	42.25
CSF	0.909	3.701	1.978	20.33
Brain	0.915	5.509	2.364	25.26

HeadExp collaborative research action

Surfacic meshes: mesh M1 (top) and mesh M2 (bottom)

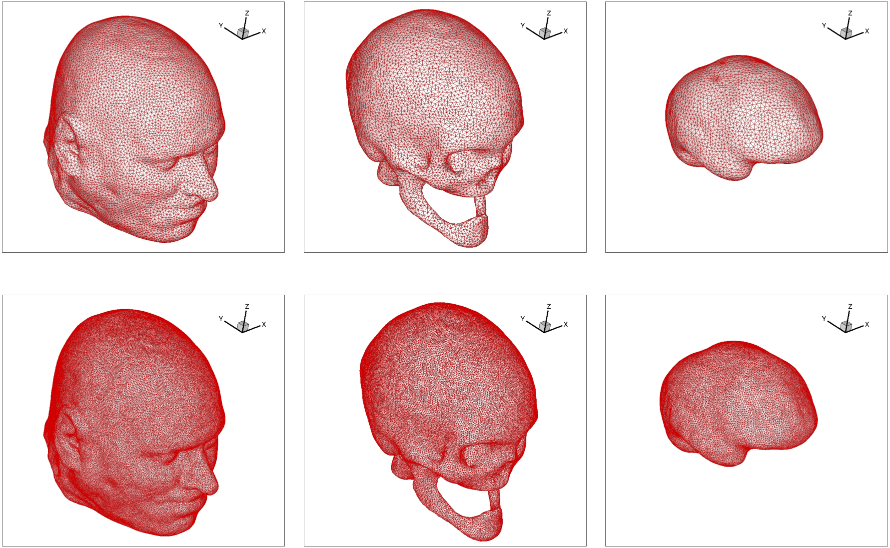

HeadExp collaborative research action

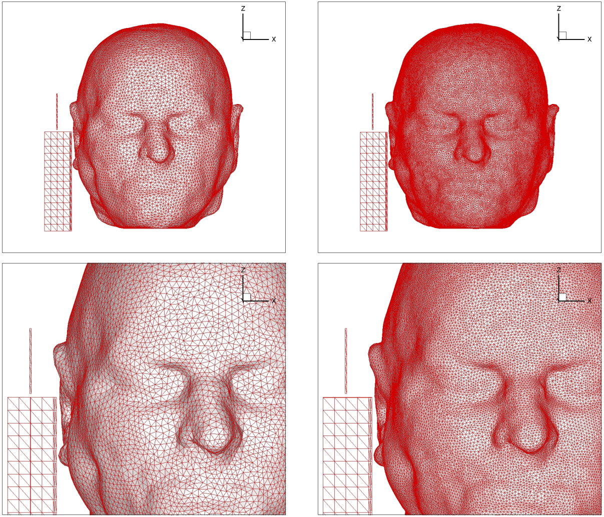

HeadExp collaborative research action

SAR (Specific Absorption Rate) : $\dfrac{\sigma|\mathbf{E}|^2}{\rho}$

SAR/SARmax (log scale)

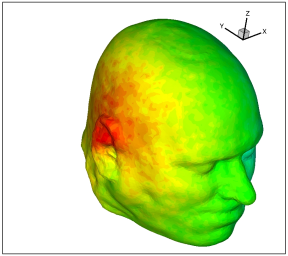

Mesh M1, $\mathbb{P}_0$-DGTD method

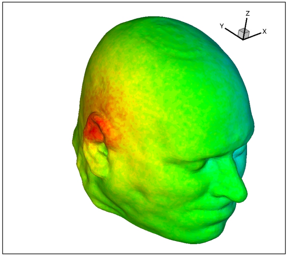

Mesh M2, $\mathbb{P}_0$-DGTD method

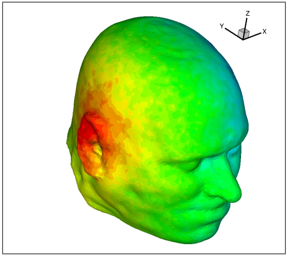

Mesh M1, $\mathbb{P}_1$-DGTD method

SAR (Specific Absorption Rate) : $\dfrac{\sigma|\mathbf{E}|^2}{\rho}$ - SAR/SARmax (log scale)

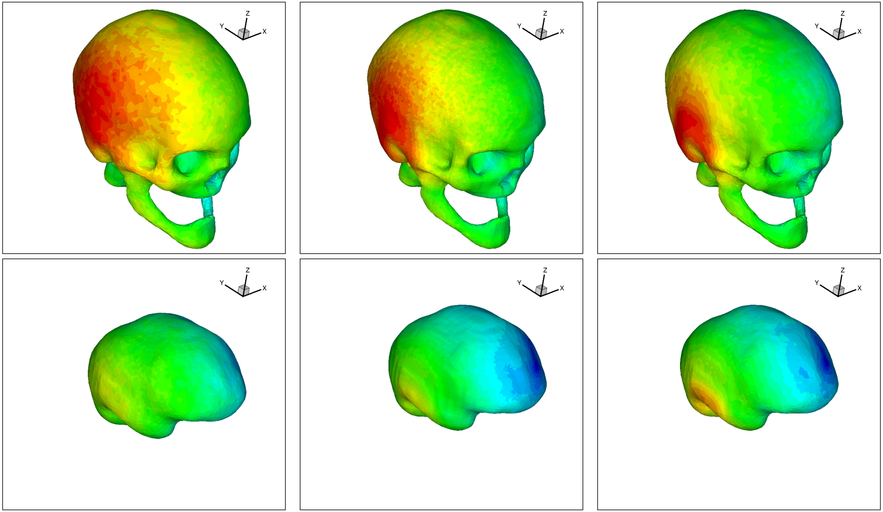

Mesh M1, $\mathbb{P}_0$-DGTD method | Mesh M2, $\mathbb{P}_0$-DGTD method | Mesh M1, $\mathbb{P}_1$-DGTD method

- AMD Opteron 2 GHz, Gigabit Ethernet

Mesh	Method	N_p	CPU	REAL	% CPU	$S(N_p)$
M1	$\mathbb{P}_0$-DGTD	32	36 mn	39 mn	92%	-
-	$\mathbb{P}_1$-DGTD	32	6 h 32 mn	6 h 48 mn	95%	-
M2	$\mathbb{P}_0$-DGTD	32	2 h 46 mn	2 h 54 mn	95%	1.00
-	-	64	1 h 20 mn	1 h 25 mn	94%	2.00

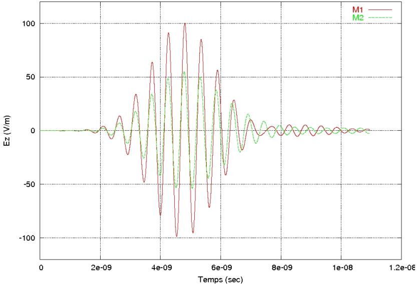

Time evolution of the E_z component

Closure

- Discontinuous Galerkin methods in summary
  - Discontinuity gives tremendous flexibility
    - Non-uniform possibly non-conforming meshes
    - Local possibly non-polynomial approximation spaces
    - *hp*-adaptivity
    - Space-time formulations
  - Discontinuity has a cost
    - Computational overhead (# degrees of freedom)
    - Stability criterion (locally refined meshes)
- Future works
  - Non-coformity (h and m)
  - Locally implicit time integration
  - Dispersive material models